


Review

Current Status of Image Recognition Technology in the Field of Corrosion Protection Applications

Xinran Wang¹ , Wei Zhang^{1,*}, Zhifeng Lin^{2,*}, Haojie Li¹, Yuanqing Zhang¹, Weiyin Quan¹, Zhiwei Chen³, Xueqiang You⁴, Yang Zeng⁵, Gang Wang³, Bolin Luo⁴ and Zhenghua Yu⁴

¹ School of Chemical Engineering and Technology, Sun Yat-sen University, Zhuhai 519000, China; wangxr67@mail2.sysu.edu.cn (X.W.)

² Jiangsu Institute of Marine Resources Development, Jiangsu Ocean University, 59 Cangwu Road, Haizhou, Lianyungang 222005, China

³ National & Local Joint Engineering Research Center of Harbor Oil & Gas Storage and Transportation Technology, Zhejiang Key Laboratory of Petrochemical Environmental Pollution Control, School of Petrochemical Engineering & Environment, Zhejiang Ocean University, Zhoushan 316022, China

⁴ Zhuhai Zhongke Huizhi Technology Co., Ltd., Zhuhai 518900, China

⁵ Zhuhai International Container Terminals (Gaolan) Co., Ltd., Zhuhai 519050, China

* Correspondence: zhangw286@mail.sysu.edu.cn (W.Z.); linzhifeng163@163.com (Z.L.)

Abstract: Corrosion brings serious losses to the economy annually. Therefore, various corrosion protection and detection techniques are widely used in the daily maintenance of large metal engineering structures. The emergence of image recognition technology has brought a more convenient and faster way for nondestructive testing. Existing image recognition technology can be divided into two categories according to the algorithm: traditional image recognition technology and image recognition technology based on deep learning. These two types of technologies have been widely used in the three fields of metal, coating, and electrochemical data images. A large amount of work has been carried out to identify defects in metals and coatings, and deep learning-based methods also show potential for identifying electrochemical data images. Matching electrochemical images with the detection of defect morphology will bring a deeper understanding of image recognition techniques for metals and coatings. A database of accumulated morphology and electrochemical parameters will make it possible to predict the life of steel and coatings using image recognition techniques.

Keywords: corrosion; nondestructive testing; image recognition; defect identification; big data



Citation: Wang, X.; Zhang, W.; Lin, Z.; Li, H.; Zhang, Y.; Quan, W.; Chen, Z.; You, X.; Zeng, Y.; Wang, G.; et al. Current Status of Image Recognition Technology in the Field of Corrosion Protection Applications. *Coatings* **2024**, *14*, 1051. <https://doi.org/10.3390/coatings14081051>

Academic Editor: Alina Vladescu

Received: 11 July 2024

Revised: 11 August 2024

Accepted: 14 August 2024

Published: 16 August 2024



Copyright: © 2024 by the authors. Licensee MDPI, Basel, Switzerland. This article is an open access article distributed under the terms and conditions of the Creative Commons Attribution (CC BY) license (<https://creativecommons.org/licenses/by/4.0/>).

1. Introduction

Corrosion, a pervasive natural phenomenon, is often referred to as “quiet destruction” due to its insidious and destructive nature. In 2014, the cost of metal corrosion in China accounted for 3.34% of the gross domestic product, approximately US \$310 billion [1]. However, with appropriate measures, 25% to 40% of corrosion losses can be prevented [2]. The ocean, which harbors vast amounts of oil, natural gas, and combustible ice, necessitates extensive offshore equipment for resource extraction. Offshore oil drilling platforms [3], transportation ships [4,5], and oil pipelines [6] are particularly susceptible to corrosion due to the high-temperature, high-humidity, and high-salinity environment of the ocean [7–9]. To mitigate corrosion, scientists have explored corrosion-resistant materials [10,11], corrosion inhibitors [12], protective coatings [13–15], and electrochemical cathodic protection [16,17]. Concurrently, engineers have employed non-destructive testing (NDT) techniques for metal corrosion detection. NDT techniques, which do not damage the inspection object, are extensively used to identify corrosion defects [18–21]. Common NDT methods include visual inspection, ultrasonic testing (UT) [22,23], pulsed eddy current testing (ECT) [24–26], and radiographic testing (RT) [27,28].

Visual inspection is the simplest and most convenient inspection method, making it widely used for detecting defects in ships, bridges, pipelines, and other facilities [29,30].

Engineers identify defects such as cracks and corrosion by sight. However, this method demands significant labor, materials, and financial resources [31]. Additionally, the identification results can vary between workers. The advent of Artificial Intelligence (AI) has introduced new approaches to corrosion detection [32–35], including image recognition as a non-destructive testing technique with the potential to replace visual inspection [36]. Engineers employ intelligent devices like drones and robots to capture corrosion images of large steel structures, enabling the efficient and accurate identification of corroded areas through computer vision. This method does not damage the inspection object and can preliminarily distinguish the type and degree of corrosion. Importantly, its evaluation is more objective, as image recognition technology can not only replicate the human eye in capturing color, shape, texture, and other features, but also quantify these data to make more accurate judgments based on predefined standards.

Image recognition techniques in corrosion protection are categorized into traditional image recognition algorithms and deep learning-based image recognition techniques [37–44]. Traditional image recognition techniques can accurately identify corrosion areas and have been widely used [42,43]. However, they rely on manually designed feature extractors, making the tuning process complex and reducing the generalization ability and robustness. By contrast, deep learning image recognition technology more precisely expresses datasets by extracting features from vast amounts of data and uncovering deeper associations between datasets [37–41]. This approach requires large datasets and powerful computing resources.

This paper primarily summarizes three aspects of image recognition technology in corrosion protection: metal, coating, and electrochemical imaging. The recognition of metals and coatings focuses on their morphological image features to distinguish between corrosion types and characteristics. The recognition of electrochemical data images involves understanding the corrosion mechanism and making predictions based on data images. Figure 1 provides an overview of the application of image recognition technology in corrosion protection.



Figure 1. Application of image recognition technology in the field of corrosion protection [24,45–49].

2. General Steps in Image Recognition Techniques

Traditional image recognition methods typically involve the following steps: image acquisition, image preprocessing, feature extraction, and image classification. Deep learning-based image recognition algorithms differ significantly. They require a large amount of labeled data, and their algorithmic architecture is more complex. Figure 2 illustrates the flowcharts of both methods.

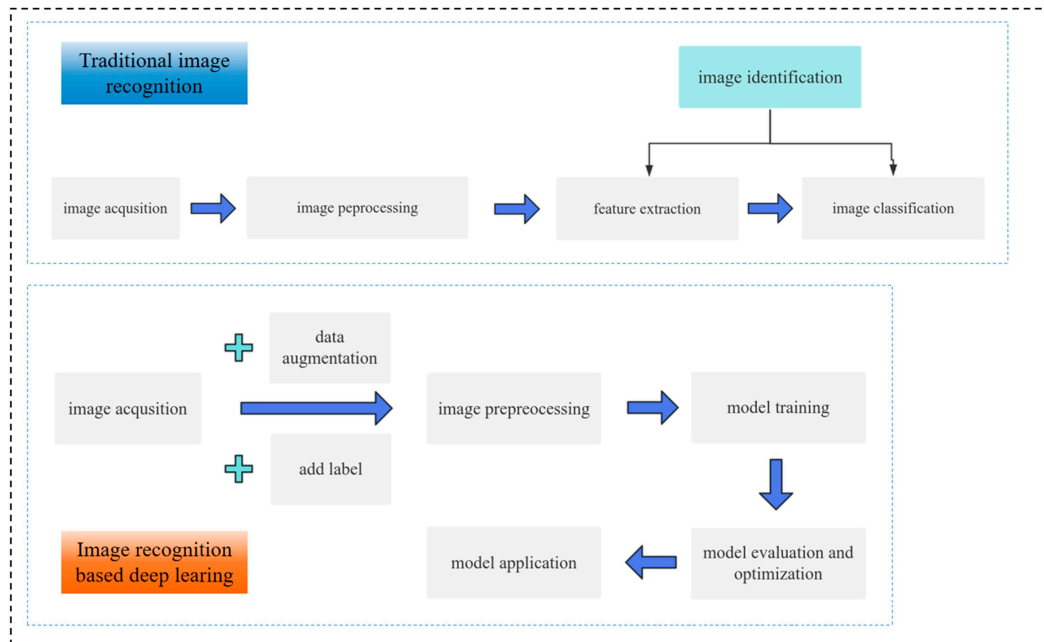


Figure 2. Flowcharts of traditional image recognition techniques and deep learning-based image recognition techniques.

2.1. Traditional Image Recognition Steps

2.1.1. Image Acquisition Collection

Three main types of capture devices are used in image recognition technology: video cameras, digital cameras, and scanning instruments (such as scanning electron microscopes and scanning acoustic microscopes). These devices can extract digital images (including moving images) through sampling, and storing the color, shape, texture, and external sounds of the pictures in computer equipment. Image acquisition is the first step in image recognition, and the quality of the acquired image affects recognition accuracy.

The quality of an image is generally related to the pixels, resolution, and DPI (dots per inch) of the capture device. Pixels, the smallest units, can only display one color. The larger each pixel, the fewer pixels can be displayed per unit area. Resolution refers to the number of pixels contained in an image, while DPI measures the number of pixels per inch (1 inch = 25.4 mm) along the length of the image. Therefore, a higher resolution and DPI typically result in higher image quality, providing more information.

In addition to image quality and clarity, the type of image also affects the choice of recognition method. Common image types for corrosion recognition include color images, grayscale images, and black-and-white images. Color images are the most commonly used and can be employed in both traditional and deep learning image recognition algorithms. Grayscale and black-and-white images are often derived from color images, although some scanning instruments, such as scanning electron microscopes, can directly capture grayscale images.

2.1.2. Image Pre-Processing

Image preprocessing aims to segment objects in the picture, eliminating unnecessary information and focusing on the data required for research. This step is crucial before feature extraction. The task can be accomplished by utilizing either Matlab R2024a or OpenCV 4.0, both of which offer a variety of functional toolkits specifically designed for image recognition. Common preprocessing methods include image binarization, noise reduction, enhancement, and geometric transformation. Image binarization is essential for traditional image recognition algorithms, converting the grayscale values of an image into binary (0 and 255) using a specific threshold, facilitating key information extraction. Noise reduction minimizes interference, while enhancement highlights critical features to improve image quality. Noise reduction is typically achieved through filtering methods, including average, median, high-pass, and low-pass filtering. Image enhancement techniques vary widely, such as contrast adjustment, sharpening, color adjustment, erosion, and dilation. Geometric transformations, like flipping, panning, rotating, and scaling, do not alter image information but help computers better understand the picture. These transformations also increase the amount of image data for more effective deep learning training.

2.1.3. Feature Extraction

Computers process images as numbers, so feature extraction involves obtaining information about these numerical or vector data through specific algorithms. Features such as color, brightness, edges, and texture can be extracted. Various image features, including edges, corners, ridges, and regions, are used to recognize different types of corrosion. Feature extraction methods are categorized based on the processing approach, including texture-based methods [50,51], color-based methods [52], edge-based methods [44], grayscale-based methods [45], and model transformation-based methods [23,53].

2.1.4. Image Classification

The core task of image classification is to assign a corresponding label to the picture. Once processed, the image feature data or vectors are classified using labels through a classifier. Traditional image recognition algorithms commonly use classifiers such as Support Vector Machines (SVM) and Random Forests (RF) [46]. The SVM classifier can perform binary classification and is a linear judgment method used for tasks such as determining whether there is corrosion in an area. Random forests is a more complex discrimination system, which can judge very complex problems by judging the results predicted by multiple decision trees. As the most widely used classifier, SVM is especially suitable for the classification of small- and medium-sized complex datasets, so its effect is better than traditional algorithms.

2.2. Deep Learning-Based Image Recognition

Deep learning-based image recognition involves four main steps: image acquisition, preprocessing, model training, and application. It utilizes convolutional neural networks (CNNs) to extract high-level features from images, requiring large datasets with accurately labeled images. The common classification architectures for deep learning include AlexNet, VGG, and ResNet. Deep learning can address both simple corrosion problems, such as defects in steel plates and coatings, and the complex image analysis of corrosion data [47,54].

3. Identification of Metals

3.1. Traditional Methods

Traditional image processing algorithms rely heavily on manually designed feature extractors, which can meet various needs and have mature application techniques, but they are also susceptible to interference and noise [55]. By contrast, deep learning can automatically learn image features during the training process without manual feature design, offering stronger generalization capabilities. Common traditional methods include wavelet variation-based methods, fractal theory-based methods, and grayscale image-based

methods. Table 1 summarizes traditional algorithms for metal recognition, while Table 2 outlines their advantages and disadvantages.

Table 1. Summary of image recognition based on conventional algorithms.

Method	Materials	Main Content	Author/Ref.	Year
Method based on wavelet transform	Al 7075-T76	The electrochemical noise signal was analyzed to reveal the characteristics of the potential signal in detail and monitor the occurrence of local corrosion	Liu [23]	2001
	Aero-aluminum alloy	The formation and growth of corrosion pits were modeled and simulated. The corroded panels were evaluated by wavelet-based image processing	Pidaparti [53]	2007
	Weathering steel	The corrosion state of weathering-resistant steel was evaluated by combining wavelet transform with the PSO-SVM technique	Yan [50]	2014
Methods based on fractal theory	Inconel alloy 600	The fractal dimension of pitting pits hardly changes with temperature	Park [56]	2003
	Reinforced Concrete (RC)	The relationship between the crack fractal dimension, corrosion rate and steel bar diameter was established to evaluate the corrosion behavior of steel bars in degraded reinforced concrete structures	Li [57]	2022
	X80 steel	The two-dimensional/three-dimensional fractal dimension of corrosion pit increased with the increase of AC density, showing linear and exponential relationships, respectively	Fu [58]	2019
Method based on grayscale	Galvanized high strength steel	The elliptic parameters of the binary image of the corrosion pit were extracted, and it was found that the elliptic parameters of the corrosion pit satisfy the Gaussian distribution along all directions	Xu [59]	2016

Table 2. Advantages and disadvantages of image recognition based on traditional algorithms.

Method	Advantage	Disadvantage
Methods based on wavelet variations	The low-frequency region responds to the color spatial distribution and brightness differences of the image, while the high-frequency region is able to respond to the local features of corrosion.	Differences in the calculation of wavelet energy entropy may lead to differences in corrosion image processing
Approach based on typing theory	It has the ability to recognize features of non-traditional Euclidean geometry in an image and to distinguish differences in roughness in image information.	The fractal dimension may be the same for different images and cannot be used alone as a criterion for judging images

Table 2. Cont.

Method	Advantage	Disadvantage
Gray scale image based approach	It has the ability to reduce complexity, increase computing speed, and improve detail clarity.	Incomplete representation of information and inability to process corrosion with color characteristics

3.1.1. Wavelet Transform-Based Approach

Wavelet transform, an image processing algorithm, decomposes an image into multiple sub-images by transforming the image's time domain into the frequency domain, enabling better feature extraction. Electrochemical noise signals can be studied using metal corrosion textures [50,51], wavelet transforms [23], corrosion pits [53], and more. Yan [50] assessed the corrosion state of weathering steel bridges using wavelet variations on corrosion texture images. Jahanshahi [51] evaluated the effect of parameters such as the color space, color channel, and sub-image block size on the color wavelet-based texture analysis algorithm to detect corrosion properties. Liu [23] used wavelet transform to decompose electrochemical noise signals into a series of sub-signals in the time–frequency domain to study localized corrosion. Pidaparti [53] evaluated the corrosion damage of aerospace materials using wavelet transform processing, investigating material loss and residual strength prediction with Artificial Neural Networks (ANNs). Based on this, ANN-based life prediction under corrosion fatigue conditions was also accomplished.

Wavelet transform can effectively extract the features of time–frequency maps of corrosion images. The low-frequency region corresponds to the color spatial distribution and brightness differences of the image, while the high-frequency region responds to the local features of corrosion. However, differences in the calculation of wavelet energy entropy may lead to variations in corrosion image processing. Additionally, the acquisition of corrosion image features by wavelet methods is often affected by the dataset size.

3.1.2. Approaches Based on Fractal Theory

The structural features in corrosion images often do not conform to traditional Euclidean geometry, and fractal theory can describe these irregular shapes effectively. Therefore, the features of each localized corrosion region can be extracted using fractal theory. By studying the fractal dimension of corrosion images, researchers can analyze the corrosion development pattern of steel, the growth change of corrosion pits, and the corrosion rate of reinforced concrete [56–58]. Park [56] studied the fractal dimension of SEM (scanning electron microscope) images of corrosion pits using fractal theory and found that the fractal dimension increases with increasing solution temperatures. The growth of corrosion pits at different solution temperatures satisfies certain fractal geometric features. Li [57] used the fractal dimension of the cracked shape of reinforced concrete surfaces to study the relationship between the cracked texture and the corrosion rate and diameter size of reinforced concrete prisms. He found that the fractal dimension was closely related to the corrosion rate and the diameter of the reinforcement. Fu [58] studied the effect of different alternating current densities on the development of the corrosion morphology of X80 steel in a coastal soil solution. He found that at low alternating current densities, X80 steel was mainly corroded uniformly; when the alternating current density reached 150 A/m², the corrosion morphology gradually transformed into irregular pitting corrosion, and the two-dimensional/three-dimensional fractal dimensions increased linearly and exponentially, respectively, with the increase in alternating current density. Fractal theory can identify the features of non-traditional Euclidean geometry in images and detect roughness differences in image information. However, it often cannot be used alone as a criterion for judging images, because the fractal dimension may be the same for different images.

3.1.3. Methods Based on Grayscale Images

Grayscale-based image processing is also a common method, utilizing differences in the gray values of images to determine the optimal gray threshold and create a binary image. Zhu et al. [24] used scanning acoustic microscopy (SAM) in C-mode with tomographic acoustic microimaging (TAMI) to determine the morphology and depth of corrosion pits on 7050 aluminum alloy. They examined the results using an optical microscope and calculated the pitting area using a binary image. Figure 3 shows the results of the binary calculation. Additionally, they plotted the 3D morphology of an aluminum alloy sample after removing the corrosion products (Figure 4) to visualize the difference in the distribution of the corrosion depth. The area share of defective areas (such as cracks) can be clearly extracted using the binarized image. Xu et al. [59] proposed an image processing-based method for the visual modeling of pits on the surface of high-strength steel wires by binarizing the image of the pit depth and extracting the parameters of corrosion ellipses. They statistically found that the direction of the long axis of the pits on the corroded surface is consistent with the circumferential direction and that the planar geometric features satisfy the Gaussian distribution. Qian et al. [60] investigated the image differences in corrosion morphology of AerMet100 Steel at different corrosion stages. They preprocessed the original images using median filtering, grayscale variation, and fuzzy enhancement. After determining the optimal threshold for image binarization, they extracted image features to calculate the degree of corrosion based on the separation theory grayscale threshold calculation method. It was found that AerMet100 Steel (a high-strength martensitic alloy steel) initially showed pitting corrosion in the accelerated test, which then gradually developed into uniform corrosion.

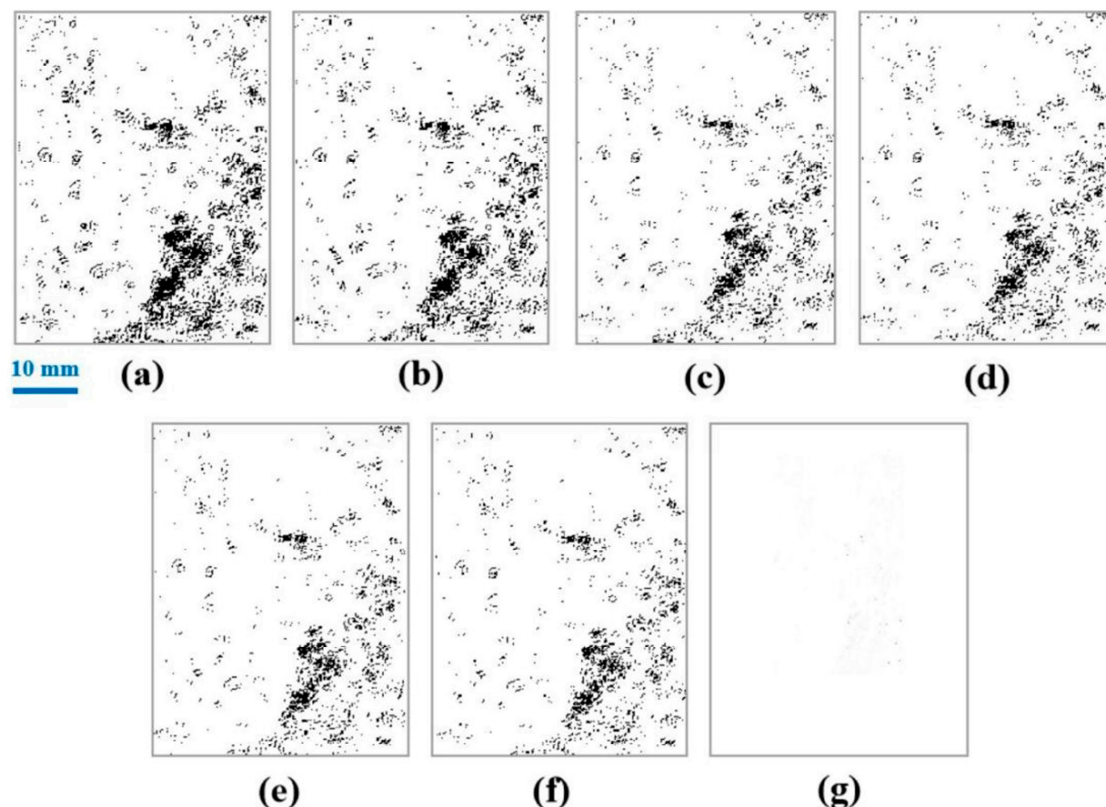


Figure 3. Binary image processing of SAM image of 7050 aluminum alloy under TAMI scanning [24] (setting all the gray values of the bright spots to 0 and all the gray values of the other points to 1); (a–g) are the layered images with depths of 51.0, 76.5, 102.0, 127.5, 153.0, 178.5, and 204.0 μm , respectively.

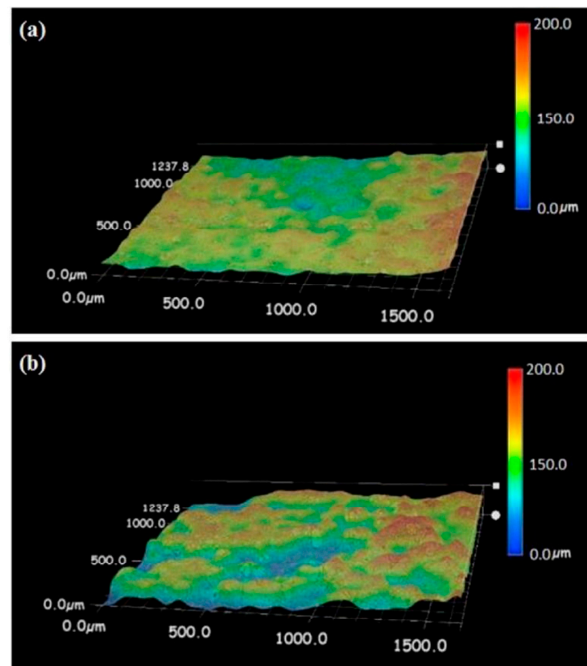


Figure 4. 3D image of 7050 aluminum alloy sample after removal of corrosion products [24]. (a) Upper-left region; (b) lower-right region.

3.2. Deep Learning-Based Approach

Algorithms used for metal image recognition are often enhanced versions of Convolutional Neural Networks (CNNs). These optimized models effectively identify and detect crack defects on metal surfaces. For instance, Zhao [61] improved the Faster R-CNN algorithm by reconfiguring the network structure and introducing multi-scale fusion and deformable convolutional networks. This enhancement increased the detection accuracy of steel surface defects to an average of 0.752, which is 0.128 higher than the original algorithm. Similarly, Xiao et al. [54] detected zinc bloom defects on galvanized steel surfaces by combining the Transformer model with the YOLO-v5 backbone feature extraction network. Figure 5a–c illustrate the architecture, recognition performance, and results of this hybrid algorithm, YOLOv5-TB. By employing a weighted bidirectional feature pyramid network (Bi-FPN) for multi-scale feature fusion, the YOLOv5-TB model surpasses most existing mainstream target-detection algorithms in both detection accuracy and efficiency.

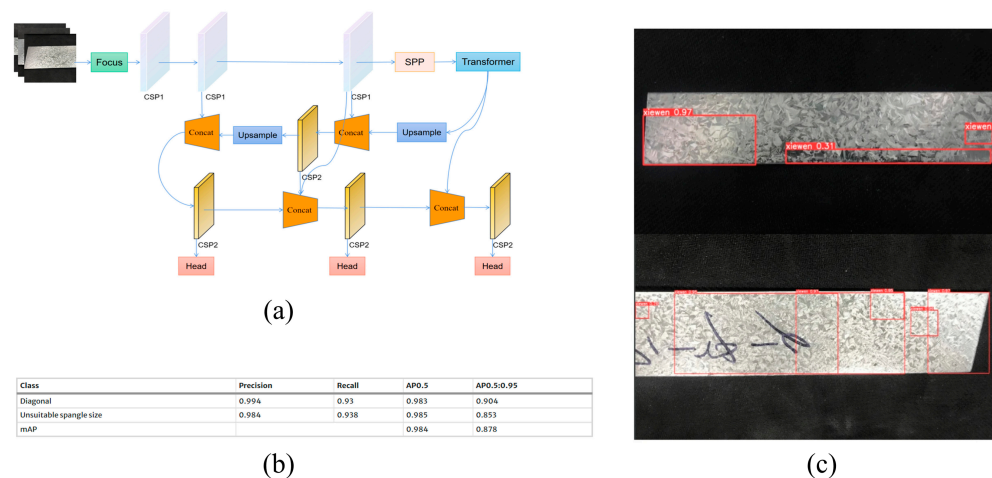


Figure 5. (a) YOLOv5-TB algorithm architecture; (b) experimental data of YOLOv5-TB algorithm defects; (c) effectiveness of this algorithm for detecting diagonal defects [54].

4. Recognition and Mining of Corrosion Data Images

Corrosion detection of coatings, a phenomenon influenced by various factors, can be approached through multiple methods. Electrochemical Impedance Spectroscopy (EIS) is an ideal non-destructive testing method that captures information about the electrochemical reactions caused by coating damage. The magnitude of the modal value reflects the protective performance of the coating and supports coating life prediction. Machine learning methods can analyze EIS spectra effectively. Ma et al. [46] proposed a method for predicting the lifetime of multilayer Cr/GLC coatings using in situ EIS data, combined with an established equation linking the coating impedance and lifetime. Their modified mechanistic–empirical model demonstrated that low-frequency impedance and the exposure time of multilayer Cr/GLC coatings at different hydrostatic pressures follow a linear empirical relationship. This combined approach of mechanistic–empirical methods and mechanistic-learning models effectively differentiates various types of electrochemical impedance spectra, correlating the coating performance with coating life. The overall structure of this model is shown in Figure 6. A comparative analysis of multiple models revealed that the ANN + RF integrated machine learning model achieved the highest combined prediction accuracy of 97.9% for coating performance and lifetime, as illustrated in Figure 7.

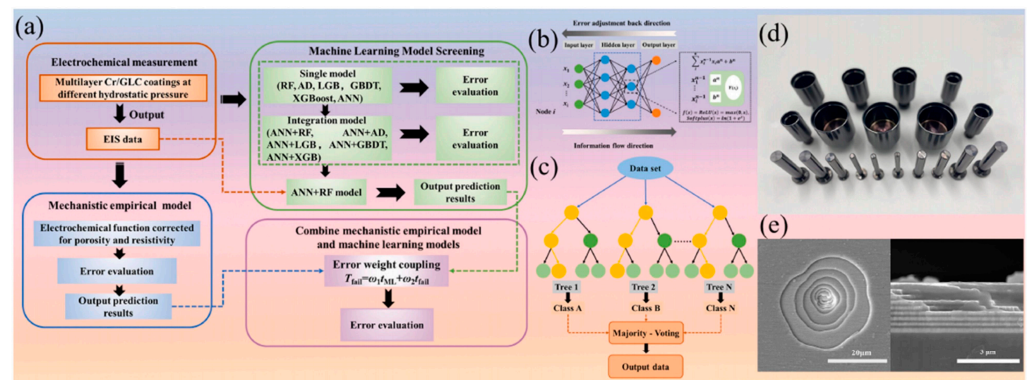


Figure 6. (a) Schematic of the process of synthesizing the empirical method of the mechanism and a machine learning model; (b) schematic of the BP-ANN algorithm; (c) schematic of the RF algorithm; (d) multi-layer Cr/GLC coatings on the sub-surface of a plunger; (e) the surface morphology of the multilayered Cr/GLC coatings; and (f) cross-sectional morphology [46].

EIS analysis is challenging because different corrosion types correspond to different equivalent circuits. It requires a deep understanding of corrosion reactions to build appropriate equivalent circuit diagrams and fit corresponding parameters using computational software. Some studies have attempted to analyze electrochemical impedance spectra with machine learning models to identify their corresponding equivalent circuits. Bongiorno et al. [47] investigated the effect of the dataset size on the parsing performance of machine learning models, considering classification and fitting cases. The training and test datasets were numerically simulated using the Labview™ programming language and a large number of EIS spectra were generated using an in-house developed program. First, an equivalent circuit was determined, then the range of fitting parameter values was given, the data were randomly selected and allocated to the circuit components, and then their equivalent circuit was simulated. They found that a dataset of 200 samples is sufficient for training models with up to five equivalent circuit components. When used for fitting, the model achieved 95% accuracy with high recall. For classification, the accuracy was around 75%, though recall varied significantly across different circuits.

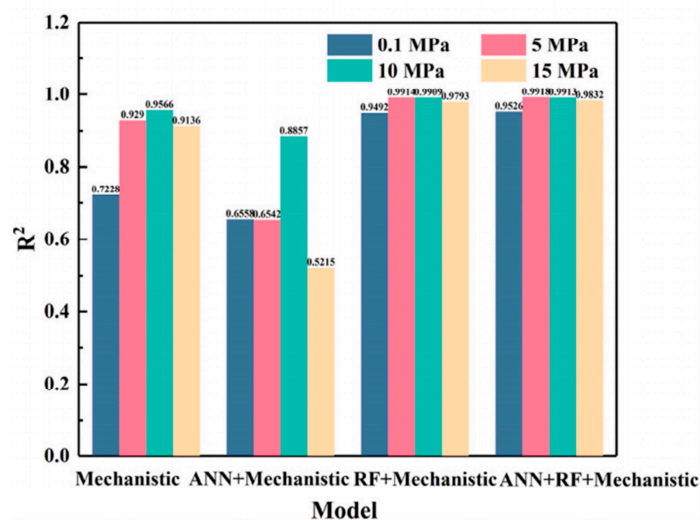


Figure 7. Evaluation metrics for the empirical model of the mechanistic model, ANN + mechanistic model, RF + mechanistic model, and ANN + RF + mechanistic model R^2 [46]. 0.1 MPa, 5 MPa, 10 MPa and 15 MPa indicate that they are different “hydrostatic pressure conditions”. R^2 represents the performance indicators of the four models, with a value close to 1 indicating better performance.

5. Identification of Coatings

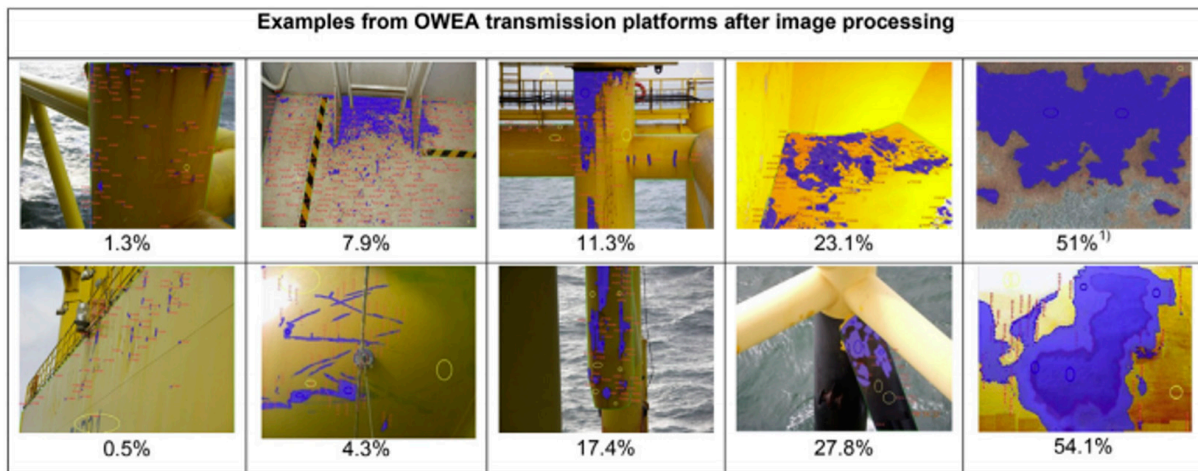
5.1. Traditional Methods

Using a computer vision system to extract specific characteristics from images of coating conditions allows engineers to assess the extent of coating corrosion more rapidly. This system can analyze the primary factors causing corrosion based on the degree of rusting and determine if recoating is necessary. Momber [52] utilized color-based digital image processing techniques to evaluate the degree of coating deterioration. Figure 8a illustrates the image recognition results for some coating areas on an offshore wind energy device, while Figure 8b shows the color changes in the coating, indicating equipment coating deterioration. In this figure, labels 1 and 2 represent the color distribution of a new coating, whereas labels 3 and 4 fall outside the acceptable range, signaling that the coating does not meet the specifications. Figure 8c presents the HSV (Hue–Saturation–Value) histogram of the corroded area, where the distribution differences in these features distinguish between heavy and light rust. The analysis of the damage causes, corresponding to each image type, revealed that most coating damage is due to inappropriate structural design and mechanical loading.

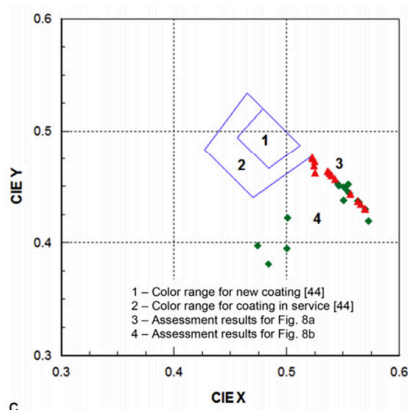
Monitoring coating quality is another critical application. Lu et al. [44] developed a hybrid algorithmic framework that effectively recognizes three different thermal barrier coating (TBC) images. By integrating image analysis techniques with statistical methods, their model accurately identifies the upper and lower boundaries of the TCL layer and generates masks for TBC images. This method achieved a classification accuracy of 98% for identifying these boundaries. Accurately differentiating the coating boundary helps calculate the coating’s porosity. Compared to their previous porosity measurement method based on adaptive local thresholding [62], the new algorithm extends the range of TBC species recognized.

Detecting the damage morphology on coating surfaces is also significant for evaluation. Blistering, a common coating defect, is primarily detected through visual inspection, which is labor-intensive and time-consuming. Machine learning algorithms enable computers to detect broken coating layers efficiently. ISO 4628-2 [63] provides standard images for grading the size and frequency of blistering using image methods, forming a basis for monitoring coating surface aging with artificial intelligence. Nadia Moradi et al. [45] created a three-dimensional graph of pixel gradient variations in blistered coatings by analyzing the reflected light differences from blistered areas, as shown in Figure 9a. Their

method separately detects large and small blisters to accurately assess various blister sizes. Subsequently, the frequency of bulges in the entire image is calculated and compared with standard image frequencies to determine its rating. Figure 9b displays the calculated frequency for the standard image, and Figure 9c shows the coating rating results using this method compared with manual ratings. The algorithm achieves a 95% identification accuracy for blisters larger than 5 mm in diameter, surpassing manual visual monitoring methods. It effectively identifies white and light gray coating blisters but is less effective for dark gray and black coatings.



(a)



(b)

Rust type / HSV values	Image	HSV histogram ¹⁾
Light rust H = peak at 10 (14°) S = 41 (16%) V = 147 (57%)		
Heavy atmospheric rust H = peak at 3 (4°) S = 156 (61%) V = 110 (42%)		

(c)

Figure 8. Effectiveness of coating evaluation on Offshore Wind Energy Installation (OWEA) [52]. (a) Example of evaluating the coating condition with digital image processing techniques; the numbers below the picture indicate the degree of coating deterioration. (b) Coating color chart. (c) Histogram of HSV for two steel corrosion stages.

Image recognition can also simultaneously detect coating defects and corrosion in steel plates. Po-Han Chen et al. [64] implemented image recognition technology to evaluate the effectiveness of steel bridge coatings. They used multi-resolution pattern classification (MPC) to identify rust and calculate defect percentages, determining whether the coating quality meets acceptance criteria. This method offers a more accurate means of detection.

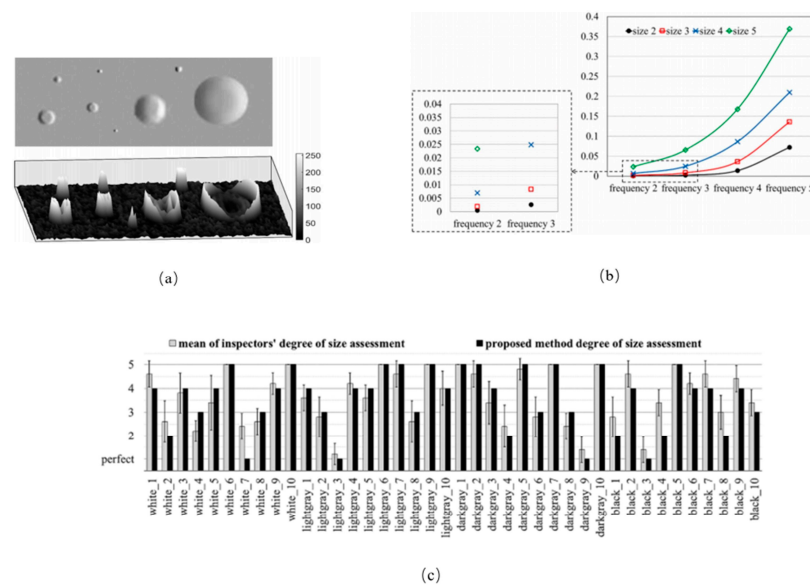


Figure 9. Identification of coating bubbles [45]. (a) 3D graph of the blister image and its gradient magnitude. Because of the differences in the intensity of the reflected light from the bubbles of different sizes, the image can be drawn based on their grayscale gradient changes. (b) Frequency criterion values used by the algorithm for grading standardized images according to ISO 4628. They are found by calculating the proportion of differently sized bubbles in the standard image proposed in [63] to the image area. (c) Comparison of the mean value of the inspector size assessment with the sample size assessment algorithm. Error bars indicate the standard deviation of the inspector results.

5.2. Deep Learning Image Recognition Algorithm

Deep learning-based methods require clear labeling of coating images to accurately determine the coating quality and types of damage. Hu et al. [65] improved the SSEResNet101 regression model to predict surface roughness through images using feature fusion methods based on the SSEResNet101 backbone. Additionally, they developed an enhanced Cascade R-CNN model that effectively identifies flame changes produced during the laser cleaning of aircraft coatings, allowing for the precise evaluation of cleaning quality. The mean square error (MSE) loss during the SSEResNet101 model training was 0.0249, and the mean absolute error (MAE) was 0.278 μm . The improved Cascade R-CNN model achieved a mean accuracy (mAP) value of 93.6% at an intersection over union (IoU) of 0.6. Several studies have utilized CNN networks for the multi-layer extraction of the morphological features of coatings. Liu et al. [66] developed an intelligent evaluation system that includes a region-based convolutional neural network (FAST R-CNN) and a deep migratory learning Vgg19 model, which efficiently identifies coating breakdown and corrosion (CBC) on surfaces, edges, and welds. Holm [67] compared the performance of different convolutional neural networks (CNNs) for automatically classifying bridge structural corrosion and coating damage in images. The VGG-16-trained convolutional neural network demonstrated the best overall performance, with recall, precision, accuracy, and F1 scores of 95.45%, 95.61%, 97.74%, and 95.53%, respectively.

Convolutional neural networks are adept at extracting the surface topography and thickness features of coatings, which can be compared with data from electrochemical tests. Samide et al. [68] conducted electrochemical tests with scanning electron microscopy (SEM) observations on PVA and nAg/PVA coatings immersed in 0.1 mol-L-1 HCl solution. Their image features were extracted using convolutional neural networks to evaluate the performance of PVA and nAg/PVA in retarding copper corrosion. The CNN data were compared with results from electrochemical measurements and SEM, showing high surface coverage in the presence of PVA (0.94) and nAg/PVA (0.98). Schmitz et al. [69] combined FEA numerical simulations with a deep learning approach to characterize coating thickness

and uniformity through dispersion curves. Features were extracted by transforming transient guided waves into dispersion plots, showing feasibility for classifying coating thickness. Yu et al. [70] proposed a novel method combining a deep convolutional neural network (CNN) with an improved data fusion approach based on Dempster–Shafer (D-S) theory to evaluate corrosion and coating defects in coal transmission and washing plants. This method accurately recognizes coating defects and is robust against various types and intensities of noise interference.

These advancements in deep learning algorithms significantly enhance the ability to detect and analyze coating defects and corrosion, providing more precise and efficient tools for maintaining structural integrity. Table 3 summarizes traditional and deep learning methods for coating identification.

Table 3. Summary of image recognition methods of coatings.

Method	Concrete Algorithm	Materials	Main Content	Ref.
Traditional method	Method based on grayscale	Alkyd paint	The bubble size and area ratio are determined based on the gray image, so as to determine the bubble grade	[45]
	Method based on color space	Coatings on offshore wind platforms	Quantitative recording and rating of coating deterioration processes	[52]
	Method based on grayscale	Coatings on steel bridge	Multiresolution pattern classification (MPC) was used to analyze the surface coating images of steel bridges, and the proportion of coating and rust in gray images was calculated	[64]
Methods based on deep learning	Deep transfer learning techniques	The coating on the ballast tank	An AI-based aided CBC evaluation system (A-CAS) was developed to identify different types of coating damage and corrosion	[66]
	Convolutional neural networks (CNN)	PVA silver nanoparticles (nAg/PVA)	The CNN data were compared with electrochemical measurements and scanning electron microscopy (SEM) data	[69]

6. Future Outlook

Current image recognition methods in the field of corrosion predominantly focus on identifying defects in steel plates and coatings. While morphological analysis helps recognize and classify various defect features and damage characteristics, it does not provide deeper insights into corrosion electrochemical information. Therefore, the analysis of corrosion data is crucial. Li [71] proposed a “corrosion big data” approach, advocating for the establishment of a standardized data warehouse for corrosion, along with data modeling and the use of this data for corrosion process simulation and experimental validation. This approach aims to simulate the corrosion process and validate it experimentally, and also suggests that corrosion data be visualized and displayed more intuitively.

Deep learning has significant potential for data image parsing. Electrochemical information obtained through testing can be visualized and displayed in images, which can then be analyzed using convolutional neural networks to extract features from various corrosion images. Linking this extracted feature information with the morphological changes in steel or coatings allows for the creation of a controlled database, enhancing the understanding of corrosion images. The application of image recognition technology can accelerate the accumulation of corrosion data and images, thereby broadening its engineering applications. By continuously linking various defect images with electrochemical images, it will be possible to establish a “corrosion big data” repository containing electrochemical information, offering great potential for predicting the lifespan of steel or coatings.

7. Conclusions

Traditional detection methods mainly rely on manual visual inspection, which is inefficient and costly, requiring significant human, material, and financial resources. By contrast, image processing technology can improve the speed and accuracy of identifying metal or coating defects. This paper summarizes the application of image recognition technology in metals, corrosion data, and coatings:

1. Traditional methods have been effectively used for detecting cracks, pitting, and other defects in steel structures. By analyzing collected images of corroded steel, extracting corrosion features, and applying mathematical methods to mine the deep features of grayscale images, it is possible to distinguish between various corrosion morphologies. However, these models often lack generalization, meaning that changes in the environment and the recognition object can greatly affect the accuracy. Additionally, selecting the right model and extracting features can be complex. Deep learning methods, which require a large number of steel surface topography images, offer a solution where different application scenarios can use the same model, albeit with different datasets.
2. By analyzing images of changes in electrochemical parameters during metal corrosion, deeper corrosion information can be extracted, such as determining equivalent circuit diagrams and predicting the lifetime of coatings.
3. Traditional image recognition methods for coatings are similar to those used for metals. However, deep learning image recognition algorithms show more potential in recognizing the boundary, thickness, and uniformity of coatings.

Combining data from electrochemical testing with image recognition technology is a promising research direction. This integration allows the results of image recognition to be supported by electrochemical information. Although it requires a substantial amount of data accumulation and workload, it offers a faster method for corrosion detection and rating.

Funding: This research was funded by the Zhuhai Industry–University–Research Cooperation Project [Grant No. 2220004002965] and National Natural Science Foundation of China [Grant Nos. 21203034 and 51771057].

Institutional Review Board Statement: Not applicable.

Informed Consent Statement: Not applicable.

Data Availability Statement: No new data were created or analyzed in this study.

Acknowledgments: The authors thank the Zhuhai Industry—University—Research Project: 2220004002965 for supporting this article.

Conflicts of Interest: Authors Xueqiang You, Bolin Luo and Zhenghua Yu were employed by Zhuhai Zhongke Huizhi Technology Co., Ltd. Author Yang Zeng was employed by Zhuhai International Container Terminals (Gaolan) Co., Ltd. The remaining authors declare that the research was conducted in the absence of any commercial or financial relationships that could be construed as a potential conflict of interest.

References

1. Hou, B.; Li, X.; Ma, X.; Du, C.; Zhang, D.; Zheng, M.; Xu, W.; Lu, D.; Ma, F. The cost of corrosion in China. *NPJ Mater. Degrad.* **2017**, *1*, 4. [[CrossRef](#)]
2. Hou, B.; Zhang, D.; Wang, P. Marine Corrosion and Protection: Current Status and Prospect. *Bull. Chin. Acad. Sci.* **2016**, *31*, 1326–1331.
3. Qiao, D.; Yan, J.; Ou, J. Fatigue analysis of deepwater hybrid mooring line under corrosion effect. *Pol. Marit. Res.* **2014**, *21*, 68–76. [[CrossRef](#)]
4. Zayed, A.; Garbatov, Y.; Guedes Soares, C. Corrosion degradation of ship hull steel plates accounting for local environmental conditions. *Ocean. Eng.* **2018**, *163*, 299–306. [[CrossRef](#)]
5. Gudze, M.T.; Melchsers, R.E. Operational based corrosion analysis in naval ships. *Corros. Sci.* **2008**, *50*, 3296–3307. [[CrossRef](#)]

6. Akhlaghi, B.; Mesghali, H.; Ehteshami, M.; Mohammadpour, J.; Salehi, F.; Abbassi, R. Predictive deep learning for pitting corrosion modeling in buried transmission pipelines. *Process. Saf. Environ. Prot.* **2023**, *174*, 320–327. [[CrossRef](#)]
7. Bhandari, J.; Khan, F.; Abbassi, R.; Garaniya, V.; Ojeda, R. Modelling of pitting corrosion in marine and offshore steel structures—A technical review. *J. Loss Prev. Process. Ind.* **2015**, *37*, 39–62. [[CrossRef](#)]
8. Alcantara, J.; de la Fuente, D.; Chico, B.; Simancas, J.; Diaz, I.; Morcillo, M. Marine Atmospheric Corrosion of Carbon Steel: A Review. *Materials* **2017**, *10*, 406. [[CrossRef](#)]
9. Huang, J.; Meng, X.; Huang, Y.; Jiang, W.; Chen, R.; Zheng, Z.; Gao, Y. Atmospheric corrosion of carbon steels in tropical and subtropical climates in Southern China. *Mater. Corros. Werkst. Und Korros.* **2020**, *71*, 1400–1406. [[CrossRef](#)]
10. Lv, S.; Li, K. Semiconducting Behaviour and Corrosion Resistance of Passive Film on Corrosion-Resistant Steel Rebars. *Materials* **2022**, *15*, 7644. [[CrossRef](#)]
11. Kausar, A.; Ahmad, I.; Bocchetta, P. High-Performance Corrosion-Resistant Polymer/Graphene Nanomaterials for Biomedical Relevance. *J. Compos. Sci.* **2022**, *6*, 362. [[CrossRef](#)]
12. Wang, Q.; Wang, R.; Zhang, Q.; Zhao, C.; Zhou, X.; Zheng, H.; Zhang, R.; Sun, Y.; Yan, Z. Application of Biomass Corrosion Inhibitors in Metal Corrosion Control: A Review. *Molecules* **2023**, *28*, 2832. [[CrossRef](#)] [[PubMed](#)]
13. Li, H.; Si, S.; Yang, K.; Mao, Z.; Sun, Y.; Cao, X.; Yu, H.; Zhang, J.; Ding, C.; Liang, H.; et al. Hexafluoroisopropanol based silk fibroin coatings on AZ31 biometals with enhanced adhesion, corrosion resistance and biocompatibility. *Prog. Org. Coat.* **2023**, *184*, 107881. [[CrossRef](#)]
14. Gnedenkova, A.S.; Filonina, V.S.; Sinebryukhov, S.L.; Gnedenkova, S.V. A Superior Corrosion Protection of Mg Alloy via Smart Nontoxic Hybrid Inhibitor-Containing Coatings. *Molecules* **2023**, *28*, 2538. [[CrossRef](#)] [[PubMed](#)]
15. Yang, C.; Xu, W.; Meng, X.; Shi, X.; Shao, L.; Zeng, X.; Yang, Z.; Li, S.; Liu, Y.; Xia, X. A pH-responsive hydrophilic controlled release system based on ZIF-8 for self-healing anticorrosion application. *Chem. Eng. J.* **2021**, *415*, 128985. [[CrossRef](#)]
16. Zhang, B.; Li, L.; Zhang, Y.; Wang, J. Study on the Interference Law of AC Transmission Lines on the Cathodic Protection Potential of Long-Distance Transmission Pipelines. *Magnetochemistry* **2023**, *9*, 75. [[CrossRef](#)]
17. Erdogan, C.; Swain, G. Conceptual Sacrificial Anode Cathodic Protection Design for offshore wind monopiles. *Ocean. Eng.* **2021**, *235*, 109339. [[CrossRef](#)]
18. Gusev, B.V.; Fedotov, M.Y.; Leshchenko, V.V.; Lepikhin, A.M.; Makhutov, N.A.; Budadin, O.N. Nondestructive Testing of Offshore Subsea Pipelines and Calculation Substantiation of their Safety According to Risk Criteria. *Chem. Pet. Eng.* **2023**, *58*, 776–787. [[CrossRef](#)]
19. Siang, T.W.; Akbar, M.F.; Jawad, G.N.; Yee, T.S.; Sazali, M.I.S.M. A Past, Present, and Prospective Review on Microwave Nondestructive Evaluation of Composite Coatings. *Coatings* **2021**, *11*, 913. [[CrossRef](#)]
20. Tonga, D.A.; Akbar, M.F.; Shrifan, N.H.M.M.; Jawad, G.N.; Ghazali, N.A.; Pakeer Mohamed, M.F.; Al-Gburi, A.J.A.; Ab Wahab, M.N. Nondestructive Evaluation of Fiber-Reinforced Polymer Using Microwave Techniques: A Review. *Coatings* **2023**, *13*, 590. [[CrossRef](#)]
21. Gong, W.; Akbar, M.F.; Jawad, G.N.; Mohamed, M.F.P.; Ab Wahab, M.N. Nondestructive Testing Technologies for Rail Inspection: A Review. *Coatings* **2022**, *12*, 1790. [[CrossRef](#)]
22. Wasif, R.; Tokhi, M.O.; Shirkoobi, G.; Marks, R.; Rudlin, J. Development of Permanently Installed Magnetic Eddy Current Sensor for Corrosion Monitoring of Ferromagnetic Pipelines. *Appl. Sci.* **2022**, *12*, 1037. [[CrossRef](#)]
23. Liu, X.F.; Wang, H.G.; Huang, S.J.; Gu, H.C. Analysis of electrochemical noise with wavelet transform. *Corrosion* **2001**, *57*, 843–852. [[CrossRef](#)]
24. Zhu, Y.; Wang, L.; Behnamian, Y.; Song, S.; Wang, R.; Gao, Z.; Hu, W.; Xia, D.-H. Metal pitting corrosion characterized by scanning acoustic microscopy and binary image processing. *Corros. Sci.* **2020**, *170*, 108685. [[CrossRef](#)]
25. Haigler, T. Introduction of NDT Methods and Techniques in Power Plants. *Mater. Eval.* **2020**, *78*, 1094–1096. [[CrossRef](#)]
26. He, D.; Kusano, M.; Watanabe, M. Detecting the defects of warm-sprayed Ti-6Al-4V coating using Eddy current testing method. *Ndt E Int.* **2022**, *125*, 102565. [[CrossRef](#)]
27. Movafeghi, A.; Mohammadzadeh, N.; Yahaghi, E.; Nekouei, J.; Rostami, P.; Moradi, G. Defect Detection of Industrial Radiography Images of Ammonia Pipes by a Sparse Coding Model. *J. Nondestruct. Eval.* **2018**, *37*, 3. [[CrossRef](#)]
28. Wang, C.; Li, W.; Xin, G.; Wang, Y.; Xu, S.; Fan, M. Novel method for prediction of corrosion current density of gas pipeline steel under stray current interference based on hybrid LWQPSO-NN model. *Measurement* **2022**, *200*, 111592. [[CrossRef](#)]
29. Agarwal, A.; Sharma, V.; Shukla, V.; Yadav, B.P.; Singh, R. IoT-and NDT-Based Bridge Risk Assessment and Identification. In Proceedings of the International Conference on Advances in the Field of Health, Safety, Fire, Environment, Allied Sciences and Engineering (HSFEA), Dehradun, India, 28 June 2018.
30. Camponeschi, E.T., Jr.; Crane, R.; Bandos, B. The role and use of nondestructive testing for US navy composite ship structures. *Mater. Eval.* **2007**, *65*, 752–758.
31. Fajardo, J.I.; Paltan, C.A.; Lopez, L.M.; Carrasquero, E.J. Textural analysis by means of a gray level co-occurrence matrix method. Case: Corrosion in steam piping systems. *Mater. Today Proc.* **2022**, *49*, 149–154. [[CrossRef](#)]
32. Lin, Z.; Zhang, W.; Li, J.; Yang, J.; Han, B.; Xie, P. Application of artificial intelligence (AI) in the area of corrosion protection. *Anti-Corros. Methods Mater.* **2023**, *70*, 243–251. [[CrossRef](#)]
33. Feiler, C.; Mei, D.; Vaghefinazari, B.; Wuerger, T.; Meissner, R.H.; Luthringer-Feyerabend, B.J.C.; Winkler, D.A.; Zheludkevich, M.L.; Lamaka, S.V. In silico screening of modulators of magnesium dissolution. *Corros. Sci.* **2020**, *163*, 108245. [[CrossRef](#)]

34. Chae, Y.H.; Kim, S.G.; Kim, H.; Kim, J.T.; Seong, P.H. A methodology for diagnosing FAC induced pipe thinning using accelerometers and deep learning models. *Ann. Nucl. Energy* **2020**, *143*, 107501. [[CrossRef](#)]
35. Zhi, Y.; Yang, T.; Fu, D. An improved deep forest model for forecasting the outdoor atmospheric corrosion rate of low-alloy steels. *J. Mater. Sci. Technol.* **2020**, *49*, 202–210. [[CrossRef](#)]
36. Naladala, I.; Raju, A.; Aishwarya, C.; Koolagudi, S.G. Corrosion Damage Identification and Lifetime Estimation of Ship Parts using Image Processing. In Proceedings of the 7th International Conference on Computing, Communications and Informatics (ICACCI), Bangalore, India, 19–22 September 2018; pp. 678–683.
37. Jin Lim, H.; Hwang, S.; Kim, H.; Sohn, H. Steel bridge corrosion inspection with combined vision and thermographic images. *Struct. Health Monit. Int. J.* **2021**, *20*, 3424–3435. [[CrossRef](#)]
38. Zhang, W.; Zhang, Y.; Gu, Q.; Zhao, H. Segmentation and grade evaluation of corrosion on hydraulic steel gates based on image-level labels. *J. Civ. Struct. Health Monit.* **2024**, *14*, 1141–1154. [[CrossRef](#)]
39. Xu, L.; Wang, Y.; Mo, L.; Tang, Y.; Wang, F.; Li, C. The research progress and prospect of data mining methods on corrosion prediction of oil and gas pipelines. *Eng. Fail. Anal.* **2023**, *144*, 106951. [[CrossRef](#)]
40. Nash, W.; Zheng, L.; Birbilis, N. Deep learning corrosion detection with confidence. *NPJ Mater. Degrad.* **2022**, *6*, 26. [[CrossRef](#)]
41. Dong, Y.; Pan, Y.; Wang, D.; Cheng, T. Corrosion detection and evaluation for steel wires based on a multi-vision scanning system. *Constr. Build. Mater.* **2022**, *322*, 125877. [[CrossRef](#)]
42. Momber, A. Colour-based assessment of atmospheric corrosion products, namely of flash rust, on steel. *Mater. Corros. -Werkst. Und Korros.* **2012**, *63*, 333–342. [[CrossRef](#)]
43. Wang, K.; Li, C.; Lu, J.; Nan, C.; Zhang, Q.; Zhang, H. Intelligent Evaluation of Marine Corrosion of Q420 Steel Based on Image Recognition Method. *Coatings* **2022**, *12*, 881. [[CrossRef](#)]
44. Lu, Y.; Chen, W.-B.; Wang, X.; Zimmerman, B. Fully Automatic Top Coat Layer Recognition in Thermal Barrier Coating Images. In Proceedings of the 23rd IEEE International Conference on Information Reuse and Integration for Data Science (IEEE IRI), Electr Network, San Diego, CA, USA, 9–11 August 2022; pp. 132–137.
45. Moradi, N.; Kandi, S.G.; Yahyaei, H. A new approach for detecting and grading blistering defects of coatings using a machine vision system. *Measurement* **2022**, *203*, 111954. [[CrossRef](#)]
46. Ma, H.; Qin, P.; Cui, Y.; Liu, R.; Ke, P.; Wang, F.; Liu, L. Prediction of multilayer Cr/GLC coatings degradation in deep-sea environments based on integrated mechanistic and machine learning models. *Corros. Sci.* **2023**, *224*, 111513. [[CrossRef](#)]
47. Bongiorno, V.; Gibbon, S.; Michailidou, E.; Curioni, M. Exploring the use of machine learning for interpreting electrochemical impedance spectroscopy data: Evaluation of the training dataset size. *Corros. Sci.* **2022**, *198*, 110119. [[CrossRef](#)]
48. Ali, A.A.I.M.; Jamaludin, S.; Imran, M.M.H.; Ayob, A.F.M.; Ahmad, S.Z.A.S.; Akhbar, M.F.A.; Suhrab, M.I.R.; Ramli, M.R. Computer Vision and Image Processing Approaches for Corrosion Detection. *J. Mar. Sci. Eng.* **2023**, *11*, 1954. [[CrossRef](#)]
49. Cha, Y.-J.; Choi, W.; Suh, G.; Mahmoudkhani, S.; Buyukozturk, O. Autonomous Structural Visual Inspection Using Region-Based Deep Learning for Detecting Multiple Damage Types. *Comput. Aided Civ. Infrastruct. Eng.* **2018**, *33*, 731–747. [[CrossRef](#)]
50. Yan, B.; Goto, S.; Miyamoto, A.; Zhao, H. Imaging-Based Rating for Corrosion States of Weathering Steel Using Wavelet Transform and PSO-SVM Techniques. *J. Comput. Civ. Eng.* **2014**, *28*, 04014008. [[CrossRef](#)]
51. Jahanshahi, M.R.; Masri, S.F. Effect of Color Space, Color Channels, and Sub-image Block Size on the Performance of Wavelet-based Texture Analysis Algorithms: An Application to Corrosion Detection on Steel Structures. *Comput. Civ. Eng.* **2013**, *2013*, 685–692.
52. Momber, A.W. Quantitative performance assessment of corrosion protection systems for offshore wind power transmission platforms. *Renew. Energy* **2016**, *94*, 314–327. [[CrossRef](#)]
53. Pidaparti, R.M. Structural corrosion health assessment using computational intelligence methods. *Struct. Health Monit. -Int. J.* **2007**, *6*, 245–259. [[CrossRef](#)]
54. Xiao, D.; Xie, F.T.; Gao, Y.; Li, Z.N.; Xie, H.F. A detection method of spangle defects on zinc-coated steel surfaces based on improved YOLO-v5. *Int. J. Adv. Manuf. Technol.* **2023**, *128*, 937–951. [[CrossRef](#)]
55. Wen, X.; Shan, J.; He, Y.; Song, K. Steel Surface Defect Recognition: A Survey. *Coatings* **2023**, *13*, 17. [[CrossRef](#)]
56. Park, J.J.; Pyun, S.I. Pit formation and growth of alloy 600 in Cl⁻ ion-containing thiosulphate solution at temperatures 298–573 K using fractal geometry. *Corros. Sci.* **2003**, *45*, 995–1010. [[CrossRef](#)]
57. Li, W.; Wu, M.; Shi, T.; Yang, P.; Pan, Z.; Liu, W.; Liu, J.; Yang, X. Experimental Investigation of the Relationship between Surface Crack of Concrete Cover and Corrosion Degree of Steel Bar Using Fractal Theory. *Fractal Fract.* **2022**, *6*, 325. [[CrossRef](#)]
58. Fu, Y.; Kou, J.; Du, C. Fractal characteristics of AC corrosion morphology of X80 pipeline steel in coastal soil solution. *Anti-Corros. Methods Mater.* **2019**, *66*, 868–878. [[CrossRef](#)]
59. Xu, Y.; Li, H.; Li, S.; Guan, X.; Lan, C. 3-D modelling and statistical properties of surface pits of corroded wire based on image processing technique. *Corros. Sci.* **2016**, *111*, 275–287. [[CrossRef](#)]
60. Ang, Q.; Ping, J.; Xiaoming, T.; De, W. Corrosion Damage Assessment of AerMet100 Steel Based on Image Analysis. *IOP Conf. Ser. Mater. Sci. Eng.* **2018**, *394*, 052066.
61. Zhao, W.; Chen, F.; Huang, H.; Li, D.; Cheng, W. A New Steel Defect Detection Algorithm Based on Deep Learning. *Comput. Intell. Neurosci.* **2021**, *2021*, 5592878. [[CrossRef](#)]

62. Chen, W.-B.; Lu, Y.; Gao, S.; Zhang, C.; Li, J.; Ogunbunmi, O.S.; Pradhan, L.; Ramsundar, P.; Zimmerman, B. An Automated Image Analysis Framework for Thermal Barrier Coating Porosity Measurement. In Proceedings of the IEEE First International Conference on Multimedia Big Data, Beijing, China, 20–22 April 2015.
63. EN ISO 4628-2; Paints and Varnishes-Evaluation of Degradation of Coatings-Designation of Quantity and Size of Defects, and of Intensity of Uniform Changes in Appearance-Part 2: Assessment of Degree of Blistering. *Comite Europeen de Normalisation*. 2016.
64. Chen, P.H.; Chang, Y.C.; Chang, L.M.; Doerschuk, P.C. Application of multiresolution pattern classification to steel bridge coating assessment. *J. Comput. Civ. Eng.* **2002**, *16*, 244–251. [[CrossRef](#)]
65. Hu, Q.; Wei, X.; Liang, X.; Zhou, L.; He, W.; Chang, Y.; Zhang, Q.; Li, C.; Wu, X. In-process vision monitoring methods for aircraft coating laser cleaning based on deep learning. *Opt. Lasers Eng.* **2023**, *160*, 107291. [[CrossRef](#)]
66. Liu, L.; Tan, E.; Zhen, Y.; Yin, X.J.; Cai, Z.Q. AI-facilitated Coating Corrosion Assessment System for Productivity Enhancement. In Proceedings of the 13th IEEE Conference on Industrial Electronics and Applications (ICIEA), Wuhan, China, 31 May–2 June 2018; pp. 606–610.
67. Holm, E.; Transeth, A.A.; Knudsen, O.O.; Stahl, A. Classification of Corrosion and Coating Damages on Bridge Constructions from Images using Convolutional Neural Networks. In Proceedings of the 12th International Conference on Machine Vision (ICMV), Amsterdam, The Netherlands, 16–18 November 2020.
68. Samide, A.; Stoean, R.; Stoean, C.; Tutunaru, B.; Grecu, R.; Cioatera, N. Investigation of Polymer Coatings Formed by Polyvinyl Alcohol and Silver Nanoparticles on Copper Surface in Acid Medium by Means of Deep Convolutional Neural Networks. *Coatings* **2019**, *9*, 105. [[CrossRef](#)]
69. Schmitz, M.; Kim, J.-Y.; Jacobs, L.J. Machine and deep learning for coating thickness prediction using Lamb waves. *Wave Motion* **2023**, *120*, 103137. [[CrossRef](#)]
70. Yu, Y.; Hoshyar, A.N.; Samali, B.; Zhang, G.; Rashidi, M.; Mohammadi, M. Corrosion and coating defect assessment of coal handling and preparation plants (CHPP) using an ensemble of deep convolutional neural networks and decision-level data fusion. *Neural Comput. Appl.* **2023**, *35*, 18697–18718. [[CrossRef](#)]
71. Li, X.; Zhang, D.; Liu, Z.; Li, Z.; Du, C.; Dong, C. Materials science: Sharing corrosion data. *Nature* **2015**, *527*, 441–442. [[CrossRef](#)]

Disclaimer/Publisher’s Note: The statements, opinions and data contained in all publications are solely those of the individual author(s) and contributor(s) and not of MDPI and/or the editor(s). MDPI and/or the editor(s) disclaim responsibility for any injury to people or property resulting from any ideas, methods, instructions or products referred to in the content.